

Einstein–de Haas Nanorotor

W. Izumida,^{1,*} R. Okuyama,² K. Sato,³ T. Kato,⁴ and M. Matsuo^{5,6,7,8}

¹*Department of Physics, Tohoku University, Sendai 980-8578, Japan*

²*Department of Physics, Meiji University, Kawasaki 214-8571, Japan*

³*National Institute of Technology, Sendai College, Sendai 989-3128, Japan*

⁴*Institute for Solid State Physics, University of Tokyo, Kashiwa 277-8581, Japan*

⁵*Kavli Institute for Theoretical Sciences, University of Chinese Academy of Sciences, Beijing, 100190, China.*

⁶*CAS Center for Excellence in Topological Quantum Computation,
University of Chinese Academy of Sciences, Beijing 100190, China*

⁷*Advanced Science Research Center, Japan Atomic Energy Agency, Tokai, 319-1195, Japan*

⁸*RIKEN Center for Emergent Matter Science (CEMS), Wako, Saitama 351-0198, Japan*

(Dated: April 17, 2022)

We propose a nanoscale rotor embedded between two ferromagnetic electrodes as a prototype of a nanorotor driven by spin injection. The spin-rotation coupling allows this nanorotor to continuously receive angular momentum from an injected spin under steady current flow between ferromagnetic electrodes with antiparallel magnetization configuration. We develop a quantum theory for a microscopic mechanism of this angular momentum transfer and show that a relaxation process from a precession state into a sleeping top state is crucial for the efficient driving of the nanorotor by solving the Master equation. Our work clarifies a general strategy for the efficient driving of a nanorotor.

Introduction.— A century ago, Einstein and de Haas demonstrated an angular momentum conversion phenomenon from magnetization to mechanical rotation [1], known as the Einstein–de Haas (EdH) effect. It has been observed in various magnetic systems [2] in a wide frequency range [3, 4]. The EdH effect has also been utilized to generate mechanical torsion using electron spin relaxation on nanoscale subjects [5–8], demonstrating a novel driving force for mechanical vibrations in the nanoelectromechanical systems (NEMS) [9].

Recently, mechanical rotational motion has been focused on in nanoscale subjects [10, 11]. Nano carbon systems would be suitable for realizing the nanorotor since they naturally contain the structure of the nanorotor. For instance, inner carbon nanotubes in multi-wall carbon nanotubes [12] or prolate spheroid shaped fullerenes in peapods [13], may work as the nanorotors and the outer nanotubes as the frame since the inner nano carbons are low friction from the van der Waals bonded frame [14]. However, efficient driving forces for the rotational motion are still lacking [10, 11].

In this Letter, we develop a quantum theory to describe a microscopic mechanism of a nanorotor driven by electron spin injection via the EdH effect. As a feasible setup, we consider a double-wall carbon nanotube rotor as shown in Fig. 1 (a). Such setup is experimentally available in ferromagnetic-carbon nanotube hybrid systems [15]. To induce its rotational motion by the electron spin injection, the nanorotor is embedded between two half-metallic ferromagnetic electrodes with antiparallel magnetization configuration, oriented to z and $-z$ directions for the source and drain electrodes, respectively. The rotor is driven by cyclic transitions among its three electronic states shown in Fig. 1 (b). By applying the bias voltage between the electrodes, an electron

with a spin $s_z = \hbar/2$ is added by tunneling from the left electrode into the nanorotor. This electron cannot tunnel to the drain electrode as long as its spin state remains $s_z = \hbar/2$ because there is no electronic state for the spin $s_z = \hbar/2$ in the half-metallic ferromagnetic drain. Electron accumulation by additional electron tunneling is also forbidden because of the Coulomb blockade in the nanorotor that plays a role of a quantum dot [16]. Therefore, only spin flip of the injected electron enables a continuous current flow through the rotor. Simultaneously with the single spin flipping ($s_z = \hbar/2 \rightarrow -\hbar/2$), the angular momentum \hbar transfers from the magnetic one to that of the mechanical rotational motion eventually. Therefore, the current through the nanorotor is expected to be a driving force of the rotational motion of the nanorotor in this system. To confirm the feasibility of the above idea, a concrete theory for the microscopic mechanism of the angular momentum transfer for the proposed setup is the subject in this Letter. The obtained condition for efficient driving is expected to be common in other experimental realizations.

We shall treat the mechanical rotation of the nanorotor as that of a rigid-body [17]. In the present rotor, two kinds of rigid-body motions, i.e., precession and sleeping top as observed for the classical tops, are possible at low energies (see the inset of Fig. 2). How to induce the sleeping top state, a rotational motion of the nanorotor around a principal axis (ζ) with aligning the axis with an outer axis (z), is the subject of this Letter. In our theory the process of angular momentum transfer is modeled by the spin-rotation coupling [18, 19]

$$H_{\text{SR}} = -\mathbf{s} \cdot \boldsymbol{\Omega}, \quad (1)$$

which expresses that the electron spin \mathbf{s} interacts with an effective magnetic field induced by the mechanical rotation with the angular velocity $\boldsymbol{\Omega}$. As also discussed

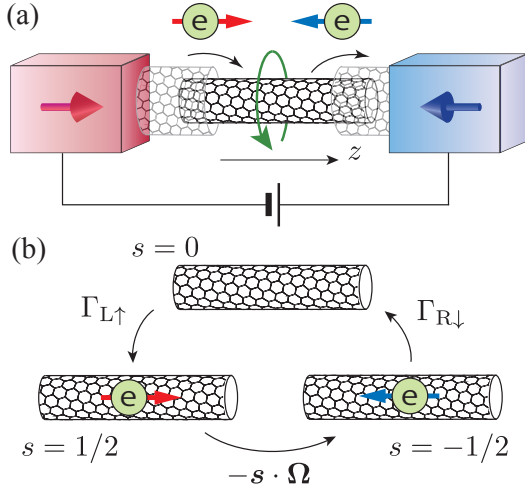


FIG. 1. (a) Schematics of the proposed structure for a nanorotor driven by spin injection. A voltage is applied to two half-metallic ferromagnetic electrodes with magnetization in the z and $-z$ directions, respectively. An electron with a spin $s_z = \hbar/2$ injected from the left electrode cannot enter the right electrode because there is no electronic state for a spin $s_z = \hbar/2$. Continuous current flow is allowed via spin flip at a rotor induced by the spin-rotation coupling that describes angular momentum transfer from a spin to the rotor. (b) Three possible electronic states of the rotor. The number of the additional electrons injected to the rotor is restricted to 0 or 1 because of the Coulomb blockade. The spin-rotation coupling is described by the Hamiltonian $-\mathbf{s} \cdot \boldsymbol{\Omega}$ and $\Gamma_{L\uparrow}(\Gamma_{R\downarrow})$ is an electron transfer rate between the rotor and the left(right) electrode.

later, a relaxation mechanism for the rotational motion to a bosonic bath with exchanges angular momentum would be incorporated to stabilize the rotational motion to the sleeping top state.

Model— Let (ξ, η, ζ) be the principal axes of inertia and (x, y, z) be the laboratory coordinate. The moments of inertia of the corresponding principal axes are denoted with $I_\xi, I_\eta,$ and I_ζ , respectively. We assume our rotor as a symmetric top with $I_\xi = I_\eta$. The rotational motion of the rotor is expressed by the following Hamiltonian [20],

$$H_R = \frac{1}{2I_\xi} \mathbf{L}^2 + \frac{1}{2} \left(\frac{1}{I_\zeta} - \frac{1}{I_\xi} \right) L_\zeta^2, \quad (2)$$

where \mathbf{L} is the angular momentum operator of the rotor, and L_ζ is the ζ component of \mathbf{L} . The Hamiltonian (2) simply expresses free rotational motion. Quantum states of the rotor, eigenstates of Eq. (2), are denoted as $|L, M, k\rangle$, which is specified by the three quantum numbers, total angular momentum $\hbar L$, its z component $\hbar M$, and ζ component $\hbar k$ [20]. To model a bearing of the rotor shaft, we shall introduce the confinement potential

$$H_{\text{pot}} = \frac{V}{2} (1 - \cos \theta), \quad (3)$$

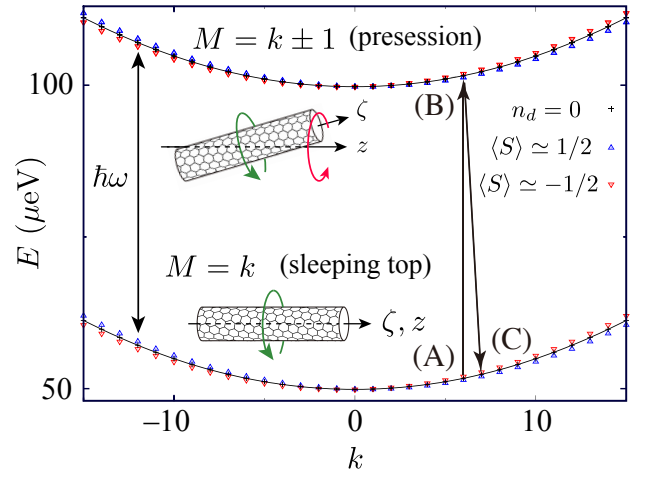


FIG. 2. Eigenenergies of rotational motion as a function of k . The upper and lower branches correspond to the precession state ($|M = k \pm 1\rangle$) and the sleeping top state ($M = k$), respectively. The insets show schematics of the corresponding rotor motions.

where $V > 0$ is the system dependent value and we may choose V to be much larger than the typical energy scale of the rotation as discussed later. The potential term has the minimum value at $\theta = 0$, where θ is the angle between the ζ and z axes. In the presence of the term H_{pot} , L is no longer conserved quantity. In the following, we use $I_\xi = I_\eta = 8.71 \times 10^4 \text{ meV} \cdot \text{ps}^2$ and $I_\zeta = 4.29 \times 10^3 \text{ meV} \cdot \text{ps}^2$, which are the values for an open end carbon nanotube defined by the two integers [16] $(n, m) = (6, 3)$ with length $L_{\text{NT}} = 4.75 \text{ nm}$, and $V = 1000 \text{ meV}$ for the potential.

The eigenstates and eigenenergies of the rotor under the potential can be calculated by diagonalizing the Hamiltonian matrices for $H_R + H_{\text{pot}}$ constructed with the basis states $|L, M, k\rangle$ by utilizing relations of the angular momentum operators and the states [21] in each (M, k) subspace. To obtain the energy spectrum, it is convenient to consider an approximation taking the leading order terms around $\theta = 0$ in the Hamiltonian. Then, the problem can be mapped to that for the two-dimensional harmonic oscillator with the angular velocity $\omega = (V/2I_\xi)^{1/2}$ [22]. Therefore, the analytical expression of the energy is given by,

$$\varepsilon_{M,k,n} = (2n + |M - k| + 1) \hbar \omega + \frac{\hbar^2 k^2}{2I_\zeta} \quad (4)$$

where $n = 0, 1, 2, \dots$ expresses the excitation in the harmonic oscillator for given M and k . Eq. (4) are shown with the solid curves in Fig. 2. The lowest branch $(M - k, n) = (0, 0)$ corresponds to the motion of sleeping top, stable rotation around the ζ axis with ζ axis aligning to the z axis. The upper branches shown in Fig. 2 correspond to the recession state $(M - k, n) = (\pm 1, 0)$ in which the angle between the z and ζ axes is kept as

constant [23]. When ω ($\propto \sqrt{V}$) is taken as sufficiently large, the each branch is energetically well separated. The sleeping top state described by the lowest branch is our target to be induced in the proposed system.

In the setup of electron transport, the nanorotor has a function of a quantum dot. The number of electrons in the nanorotor changes one by one. We shall model the electronic states in the nanorotor contributing to the transport with zero ($n_d = 0$) and single electron ($n_d = 1$). These states can be represented with the spin index as $|s\rangle$ with $s = 0$ for $n_d = 0$ and $s = \pm 1/2$ for $n_d = 1$ (see Fig. 1 (b)). The Hamiltonian for the electronic states is then written as $H_s = \sum_s \epsilon_0 n_d(s) |s\rangle \langle s|$. We shall choose $\epsilon_0 = 0$ to represent the resonant tunneling condition.

In the nanorotor, an electron spin interacts with the mechanical rotational motion via the spin-rotation coupling Eq. (1). The quantum states of the nanorotor with a single electron are exactly obtained by diagonalizing the Hamiltonian matrices for $H_R + H_{\text{pot}} + H_s + H_{sR}$. The eigenenergies are also plotted in Fig. 2, showing the small splitting of the energies between the spin up and down states as the result of the interaction. In the present model, $M + s$ and k are the conserved quantities. Therefore the spin-rotation coupling can mix the states in (M, s) and $(M + 2s, -s)$ subspaces. That is, the interaction exchanges the z component of the angular momentum between the electron and the mechanical rotation, but not the ζ component in the present setup for the symmetric top. The angular-momentum exchange processes are diagrammatically shown in Fig. 2 with the arrow between (A) and (B). The interaction mixes the states in the lowest and second branches. To induce faster sleeping top motion, running up the the lowest branch in the present setup, additional processes to mix the different k states, together with the spin-rotation coupling, are required. Therefore, as discussed later, we will include a relaxation process from the higher to the lowest branches [(B) to (C) in Fig. 2] via a bosonic bath in our model.

Rotational motion induced by spin injection.— The effect of the electrodes on the rotor states is accounted by adding the following Hamiltonian,

$$H_e = \sum_{\substack{r=R,L \\ q,s}} \epsilon_{rqs} c_{rqs}^\dagger c_{rqs} + \sum_{\substack{r=R,L \\ q,s}} V_{rqs} c_{rqs}^\dagger d_s + \text{H.c.} \quad (5)$$

The time evolution of the probability of the rotor states, w_i , is described by the Master equation

$$\frac{dw_i}{dt} = \sum_j \Gamma_{ij} w_j - \sum_j \Gamma_{ji} w_i, \quad (6)$$

where i specifies a eigenstate of the rotor system including electronic states described by $H_R + H_{\text{pot}} + H_s + H_{sR}$.

As often observed in macroscopic systems, there would exist relaxation processes, which lower energy of the rotational motion, to stabilize the motion. To account such

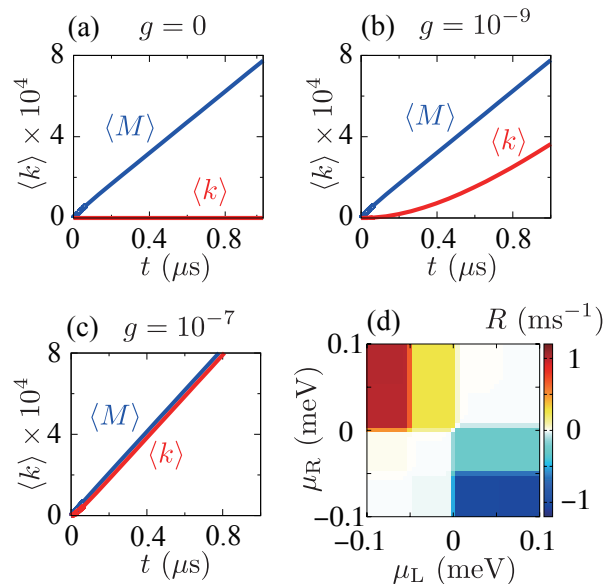


FIG. 3. Time evolutions of the rotational motion for (a) $g = 0$, (b) $g = 10^{-9}$, and (c) $g = 10^{-7}$. The chemical potentials of left and right electrodes are chosen to be $\mu_L = -\mu_R = 0.1$ meV. (d) Density plot of the rotatability in the source and drain chemical potentials, μ_L - μ_R plane.

processes, we shall explicitly consider a coupling to the bosonic bath modeled by the following Hamiltonian,

$$H_B = \sum_q \hbar \omega_q b_q^\dagger b_q + \sum_q g_q (b_{-q}^\dagger + b_q) L_+^{(\zeta)} + \text{H.c.} \quad (7)$$

where $L_+^{(\zeta)}$ ($L_-^{(\zeta)}$) is the angular momentum operator ascending (descending) the k states such as

$$L_\pm^{(\zeta)} |L, M, k\rangle = \sqrt{L(L+1) - k(k \pm 1)} |L, M, k \pm 1\rangle, \quad (8)$$

and the relaxation ratio is assumed as $\gamma^{(b)}(\varepsilon) = 2\pi g \hbar^{-1} \varepsilon \Theta(\varepsilon)$ for a Ohmic bath. As shown later, the process modeled by Eq. (7) induces the relaxation from the precession to sleeping top. The effect of the relaxation expressed by Eq. (7) will be clarified in the numerical simulation.

Numerical simulation.— Time evolution of the rotational motion is calculated by solving the differential equation of Eq. (6). The temperature is chosen as $T = 10$ mK and the thermal equilibrium state of the rotor is chosen as the initial state. The tunnel couplings are chosen as $\Gamma_{L\uparrow} = \Gamma_{R\downarrow} = 5 \times 10^{-5}$ meV, $\Gamma_{L\downarrow} = \Gamma_{R\uparrow} = 0$ to represent the ferromagnetic electrodes. The bias voltages are switched on at $t = 0$. The expected values of M and k , $\langle M \rangle$ and $\langle k \rangle$, will be shown.

The time evolution of the rotational motion in the absence of the relaxation ($g = 0$) and these with the relaxation ($g = 10^{-9}$, $g = 10^{-7}$) are shown in Fig. 3 (a)-(c). In

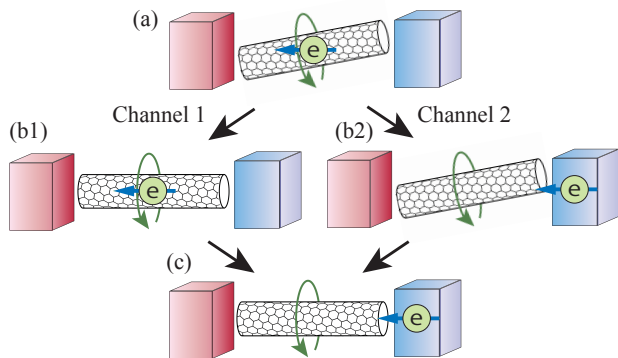


FIG. 4. Two channels that are relevant to electron transfer.

the absence of the relaxation, $\langle M \rangle$ increases almost linearly with respect to time keeping $\langle k \rangle$ almost zero. This means that the precession motion schematically represented in the upper inset of Fig. 2 is developed. In contrast, in the presence of the relaxation, $\langle k \rangle$ develop as dragged up by $\langle M \rangle$. That is, the rotation with the sleeping top state $M = k$ schematically represented in the lower inset of Fig. 2 (b) is developed. We note that the relaxation process indeed lowers the total energy by transition into the lowest branch. This result clearly show the role of the relaxation on the stabilizing the rotation to the state of the sleeping top.

As shown in Fig. 3 (a)-(c), $\langle k \rangle$ develops linearly in the long time scale for the presence of the relaxation. We shall define a rotatability R as the slope of $\langle k \rangle$ in time as follows;

$$R \equiv \lim_{t \rightarrow t_\infty} \frac{\langle k \rangle(t)}{t}, \quad (9)$$

where t_∞ is taken sufficiently long time after applying the bias voltage at which the time evolution develops linearly in time. The rotatability R can be an index for the easiness of inducing the rotation motion of the sleeping top.

Fig. 3 shows the calculated rotatability R in a wide range of the source and drain bias voltages. Since the symmetry relation $R(\mu_L, \mu_R) = -R(\mu_R, \mu_L)$ holds, let us focus on the positive bias regime ($\mu_L > \mu_R$). It is clearly shown that there exists the contribution to the rotatability in the low bias regime, $-0.05 \text{ meV} < \mu_R < 0$, and around the border $\mu_R \simeq -0.05 \text{ meV}$ the sharply becomes large. These behaviors can be understood as the number of channels of the current. A electron with $s = 1/2$ first tunnels from the left lead to the rotor, and the angler momentum transfer occurs because of the spin-rotation coupling as $(M, k, 1/2) \rightarrow (M+1, k, -1/2)$. The resultant state is shown in Fig. 4 (a). At the lower bias regime the following process mainly contributes to the current flow as shown by channel 1 in Fig. 4; (i) Relaxation $(M+1, k, -1/2) \rightarrow (M+1, k+1, -1/2)$ and (ii) the spin-flipped electron (with $s = -1/2$) tunnels

from the rotor to the right lead. In addition to channel 1, channel 2 shown in Fig. 4 opens when the bias of the right electrode, μ_R , is smaller than $-\hbar\omega$, which corresponds to the energy difference between the sleeping top and precession states.

Summary.— We have proposed a nanoscale rotor embedded between two ferromagnetic electrodes as a prototype of a nanorotor driven by injected spins via the EdH effect. As a feasible example, we considered a double-wall carbon nanotube rotor and developed a microscopic theory, where the quantum states of the nanorotor in a frame have been exactly given as these of the symmetric top under the potential. We found that the relaxation process from a precession state into a sleeping top state is crucial for the efficient driving of the nanorotor by solving the Master equation.

The mechanism discussed in the Letter is not restricted for the carbon nanotubes but is general for other materials. Further, there could exist other spin transfer processes from the electron spin, such as via spin-orbit and electron-phonon interactions, nuclear spin interaction. Then, locally deformed structure would eventually relax to the rotational motion. The process discussed in the Letter would be a minimal model for the momentum transfer from the electron to the rotor effectively including the other possible processes. The present results will offer a general strategy for the efficient driving a nanorotor in the spin-based NEMS.

We acknowledge JSPS KAKENHI Grants (Nos. JP16H01046, JP18H04282, JP19K14637, JP20K03831, JP20H01863, JP20K05258, JP21K03414). MM is partially supported by the Priority Program of Chinese Academy of Sciences, Grant No. XDB28000000.

* wizumida@tohoku.ac.jp

- [1] A. Einstein and W. J. de Haas, “Experimental proof of the existence of ampère’s molecular currents,” KNAW proc. **18 I**, 696 (1915).
- [2] GG Scott, “Review of gyromagnetic ratio experiments,” Rev. Mod. Phys. **34**, 102 (1962).
- [3] Christian Dornes, Yves Acremann, Matteo Savoini, Martin Kubli, Martin J Neugebauer, Elsa Abreu, Lucas Huber, Gabriel Lantz, Carlos AF Vaz, Henrik Lemke, *et al.*, “The ultrafast einstein–de haas effect,” Nature **565**, 209–212 (2019).
- [4] K Mori, MG Dunsmore, JE Losby, DM Jenson, M Belov, and MR Freeman, “Einstein–de haas effect at radio frequencies in and near magnetic equilibrium,” Phys. Rev. B **102**, 054415 (2020).
- [5] P. Mohanty, G. Zolfagharkhani, S. Kettemann, and P. Fulde, “Spin-mechanical device for detection and control of spin current by nanomechanical torque,” Phys. Rev. B **70**, 195301 (2004).
- [6] T. M. Wallis, J. Moreland, and P. Kabos, “Einstein–de haas effect in a nife film deposited on a microcantilever,” Appl. Phys. Lett. **89**, 122502 (2006).

- [7] Guiti Zolfagharkhani, Alexei Gaidarzhy, Pascal Degiovanni, Stefan Kettemann, Peter Fulde, and Pritiraj Mohanty, “Nanomechanical detection of itinerant electron spin flip,” *Nat Nano* **3**, 720–723 (2008).
- [8] K. Harii, Y.-J. Seo, Y. Tsutsumi, H. Chudo, K. Oyanagi, M. Matsuo, Y. Shiomi, T. Ono, S. Maekawa, and E. Saitoh, “Spin seebeck mechanical force,” *Nat. Commun.* **10**, 2616 (2019).
- [9] Andrew N. Cleland, *Foundations of Nanomechanics: From Solid-State Theory to Device Applications* (Springer, Berlin, Germany, 2003).
- [10] A. M. Fennimore, T. D. Yuzvinsky, Wei-Qiang Han, M. S. Fuhrer, J. Cumings, and A. Zettl, “Rotational actuators based on carbon nanotubes,” *Nature* **424**, 408–410 (2003).
- [11] S. W. D. Bailey, I. Amanatidis, and C. J. Lambert, “Carbon nanotube electron windmills: A novel design for nanomotors,” *Phys. Rev. Lett.* **100**, 256802 (2008).
- [12] S. Iijima, “Helical microtubules of graphitic carbon,” *Nature* **354**, 56–58 (1991).
- [13] M. Krause, M. Hulman, H. Kuzmany, O. Dubay, G. Kresse, K. Vietze, G. Seifert, C. Wang, and H. Shinohara, “Fullerene quantum gyroscope,” *Phys. Rev. Lett.* **93**, 137403 (2004).
- [14] J. Cumings and A. Zettl, “Low-friction nanoscale linear bearing realized from multiwall carbon nanotubes,” *Science* **289**, 602–604 (2000).
- [15] A Cottet, T Kontos, S Sahoo, H T Man, M-S Choi, W Belzig, C Bruder, A F Morpurgo, and C Schönenberger, “Nanospintronics with carbon nanotubes,” *Semiconductor Science and Technology* **21**, S78 – S95 (2006).
- [16] E. A. Laird, F. Kuemmeth, G. A. Steele, K. Grove-Rasmussen, J. Nygård, K. Flensberg, and L. P. Kouwenhoven, “Quantum transport in carbon nanotubes,” *Rev. Mod. Phys.* **87**, 703 (2015).
- [17] Such treatment is justified for the nano scaled subject such as a carbon nanotube with nanometer length in which typical energy scale of lattice deformation (\sim meV) is much higher than that of the rotational motion.
- [18] Friedrich W Hehl and Wei-Tou Ni, “Inertial effects of a dirac particle,” *Physical Review D* **42**, 2045 (1990).
- [19] M. Matsuo, E. Saitoh, and S. Maekawa, “Spin-mechatronics,” *Journal of the Physical Society of Japan* **86**, 011011 (2017).
- [20] L. D. Landau and E. M. Lifshitz, *Quantum Mechanics — Non-relativistic theory (Third Edition)* (Pergamon Press, Oxford, England, 1977).
- [21] L. C. Biedenharn and James D. Louck, *Angular Momentum in Quantum Physics: Theory and Application* (Cambridge University Press, Cambridge, 1984).
- [22] The coordinate θ corresponds to the radial component of the mapped two-dimensional harmonic oscillator.
- [23] The higher branches that are not shown in Fig. 2 includes the mutation state in which θ fluctuates around an average angle $\theta_0 = \sqrt{\hbar|M - k|/I_\xi\omega}$.